Proc. Natl. Acad. Sci. USA
Vol. 95, pp. 4991–4996, April 1998
Cell Biology

Localization of nascent RNA and CREB binding protein with the PML-containing nuclear body

VICKIE J. LAMORTE*†‡, JACQUELINE A. DYCK*‡§, ROBERT L. OCHS¶, AND RONALD M. EVANS*‖

*Howard Hughes Medical Institute, The Salk Institute for Biological Studies, La Jolla, CA 92037; and ¶Department of Molecular and Experimental Medicine, The Scripps Research Institute, La Jolla, CA 92037

Contributed by Ronald M. Evans, March 6, 1998

ABSTRACT **The cellular role of the PML-containing nuclear bodies also known as ND10 or PODs remains elusive despite links to oncogenesis and viral replication. Although a potential role in transcription has been considered, direct evidence has been lacking. By developing a novel *in vivo* nucleic acid labeling approach, we demonstrate the existence of nascent RNA polymerase II transcripts within this nuclear body. In addition, PML and the transactivation cofactor, CREB binding protein (CBP), colocalize within the nucleus. Furthermore, we show that CBP in contrast to PML is distributed throughout the internal core of the structure. Collectively, these findings support a role for this nuclear body in transcriptional regulation.**

The literature contains reports of the promyelocytic leukemia gene product PML protein functioning as an enhancer of transcription (1) as well as a suppressor of transcription and growth (2). As these data are limited to the dynamically distributed PML protein, we chose to focus on providing a role for the PML-containing nuclear body itself. PML was discovered through its rearrangement in the t(15:17) chromosomal translocation, where it becomes fused to the retinoic acid receptor α. This results in the production of the PML–retinoic acid receptor fusion protein, which is the presumed etiologic agent of acute promyelocytic leukemia (3–12). PML shares homology with a subset of genes of unknown function in the RING finger motif family characterized by three cysteine-rich clusters followed by a coiled-coil region (13). Three of these proteins, including PML, T18 (14), and Ret (15), participate as fusion proteins that transform through unknown mechanisms. Interestingly, two other members of this family, XNF7 (16) and pWA33 (17), both amphibian maternal factors, localize to lampbrush chromosome loops, suggesting an association with transcriptional events or resultant nascent RNA. Another member of this family, SS-A/Ro (18, 19), is found in a ribonucleoprotein complex. Thus, these prior studies suggest that PML and the PML-containing nuclear body may play a role in transcriptional events. Immunohistochemical analysis demonstrates the PML-containing nuclear body to be composed of at least four proteins, including PML, PML-associated factor (PAF31) (J. D. Chen and R.M.E., unpublished data), the SP-100 autoantigen of primary biliary cirrhosis, and the nuclear matrix protein NDP55 (20–23). Furthermore, PML-containing nuclear bodies are altered during the process of viral infection (24–26).

Like PML and its corresponding nuclear body, CBP/P300 has been shown to be a target of viral oncoproteins including the E1A adenoviral (27) and the HTLV-1 Tax oncoproteins (28). The CREB binding protein (CBP) has been shown to be a coactivator for a variety of regulatory transcriptional events (29–31). This protein has also been shown to possess acetyltransferase activity, further implicating it in the accessibility of chromatin/histones for active transcription (32, 33). Thus, we chose to establish a link between the PML-containing nuclear body and CBP.

MATERIALS AND METHODS

Cell Culture and Microinjection. HEp-2 cells cultured in DMEM with 10% heat-inactivated fetal calf serum with 1% penicillin-streptomycin (GIBCO) on etched glass coverslips (Bellco Glass) were microinjected with 1 mM fluorescein-12-uridine-5′-triphosphate (FITC–UTP) (Boehringer Mannheim) diluted in 50 mM Hepes, 20 mM NaCl, pH 7.4. Approximately 10^{-15} liters/cell was introduced into the cytoplasm using a semi-automated Eppendorf microinjection system and a Nikon inverted microscope. For PML–green fluorescent protein (GFP) expression, cells were microinjected with a CMX PML–GFP DNA expression construct at 50–200 ng/μl and incubated overnight to allow for expression.

Immunodetection of Nascent RNA. Cells were exposed to hypotonic detergent treatment to extract unincoporated FITC–UTP. It is of note that foci are also present in cells that have been immediately fixed and not subjected to extraction. Plates were washed three times in ice-cold Kern Matrix buffer (10 mM MES/10 mM NaCl/1.5 mM $MgCl_2$/10% glycerol), incubated 30 min in extraction buffer (10 mM NaCl/10 mM MES/1.5 mM $MgCl_2$/10% glycerol/1% Nonidet P-40), and washed again three times.

Cells were fixed with 4% freshly made paraformaldehyde for 30 min at ambient temperature, washed three times with PBS, and blocked for 1 h in 2% normal donkey serum. Fixed cells were labeled with affinity-purified rabbit antibodies raised against a synthetic peptide [PML (aa 1–14)] (20). Briefly, the specimens were incubated for 2 h at room temperature with primary affinity-purified anti-PML diluted 1:100 in 2% normal donkey serum, washed three times with cold PBS, and incubated for 1 h with the secondary antibody, donkey anti-rabbit IgG-rhodamine (Jackson ImmunoResearch). Antibodies to p80-coilin were used as previously described (34, 35). After rinsing in PBS, the sample was mounted in anti-quenching mountant.

Antibodies and Immunodetection. Two antibodies to PML, the affinity-purified rabbit polyclonal antibody PML (1–14 amino acids) and the 5E10 monoclonal antibody (a kind gift of

Abbreviations: PML, promyelocytic leukemia gene product; CBP, CREB binding protein; FITC, fluorescein isothiocyanate; aa, amino acid(s); pol I and II, polymerase I and II; GFP, green fluorescent protein.

†Current address: Beckman Laser Institute, Laser Microbeam & Medical Program, University of California, Irvine, CA 92612.
‡V.J.L. and J.A.D. contributed equally to this work.
§Current address: Division of Cellular and Molecular Medicine, University of California, San Diego, La Jolla, CA 92122.
‖To whom reprint requests should be addressed at: The Salk Institute for Biological Studies, Howard Hughes Medical Institute, Gene Expression Laboratory, 10010 North Torrey Pines Road, La Jolla, CA 92037. e-mail: evans@salk.edu.

The publication costs of this article were defrayed in part by page charge payment. This article must therefore be hereby marked "*advertisement*" in accordance with 18 U.S.C. §1734 solely to indicate this fact.

L. de Jong), were used to detect PML as noted. Several antisera to CBP were employed and include an affinity-purified rabbit polyclonal antibody to aa 634–648, antisera 5729 to aa 1–100, antisera 5614 to a GSTKIX fusion protein of aa 455–679, and C-20, an affinity-purified rabbit polyclonal antibody, to aa 2422–2441 (Santa Cruz Biotechnology). Appropriate secondary antibodies were used at 1:200 dilution (Jackson ImmunoResearch).

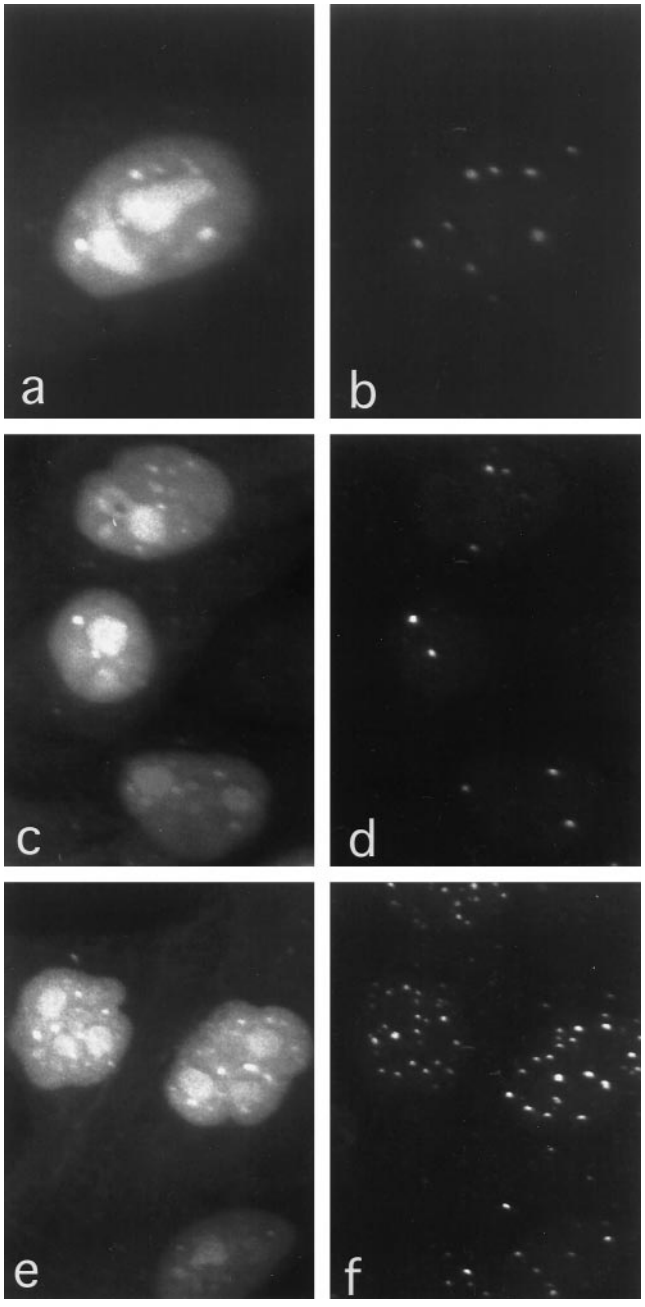

FIG. 1. Confocal microscopy of HEp-2 cells microinjected with FITC–UTP. Fluorescent labeling was localized in PML-containing nuclear bodies and in coiled bodies, both of which are nuclear bodies of unknown function. Although not all PML bodies correspond to FITC–UTP foci, all the foci can be accounted for by either PML bodies or coiled bodies. Note that nucleoli have also incorporated FITC–UTP. Some FITC-labeled foci (*a*) colocalize with some nuclear bodies labeled with an anti-PML antibody and were detected with an LRSC-conjugated secondary antibody (*b*). Some FITC–UTP foci (*c*) colocalize with coiled bodies detected with anti-p80–coilin antibodies and LRSC (*d*). Cells labeled with both anti-p80–coilin and anti-PML detected by LRSC (*f*) demonstrate that all of the FITC–UTP foci (*e*) colocalized with either PML-containing nuclear bodies or coiled bodies (*f*).

Confocal and Fluorescence Microscopy. For nascent RNA colocalization studies, samples were examined using a Zeiss Axiovert 35M equipped with a Bio-Rad MRC-600 laser-scanning confocal attachment. Dual excitation was achieved using the 488- and 568-nm lines from a krypton-argon laser. Digital images were converted to Pict files, and images were merged using ADOBE PHOTOSHOP. Standard epifluorescence microscopy was performed with a Nikon Microphot SA.

Electron Microscopy. Ultrastructural analysis was performed as previously described according to a pre-embedding technique (35). HEp-2 cells were immunolabeled with affinity-purified rabbit anti-CBP (aa 634–648) and anti-PML (aa 1–14) antibodies, which were detected utilizing Nanogold conjugated secondary antibody and a silver enhancement process. EDTA regressive staining (36), which specifically detects ribonucleic acid, was done in tandem with pre-embedding immunodetection to demonstrate the presence of RNA in the PML-containing nuclear bodies.

RESULTS

Nascent RNA Localized to the PML-Containing Nuclear Bodies. To examine a potential link between PML's homology to known RING finger proteins associated with RNA, we performed experiments to see whether PML colocalized with nascent RNA. To detect nascent or newly transcribed RNA, incorporation of Br-UTP into RNA and subsequent immunodetection have previously identified hundreds of granular-like sites of transcription that are distributed throughout the nucleoplasm (37, 38). However, this technique failed to detect any association between the PML-containing bodies and newly synthesized RNA (22, 39). As Br-UTP appears to be weakly incorporated into nucleolar RNA (presumably due to nucleolar exclusion of the labeling reagent) (37, 38), it could be reasoned that other compartmentalized RNA might be contained within a PML-containing body that may go undetected. For example, RNA in such a body may not be accessible to immunologic probes used to detect the Br moiety. In addition,

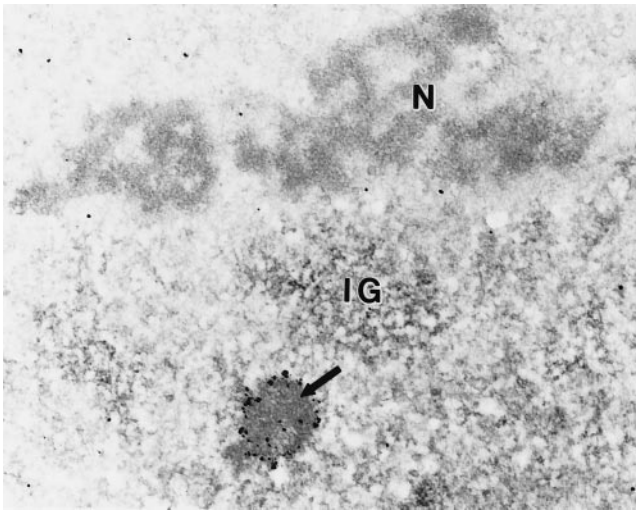

FIG. 2. Ribonucleic acid can be detected in the PML-containing nuclear bodies. Immunoelectron microscopy of a nucleus labeled for PML followed by EDTA-regressive staining (36) demonstrates the localization of RNA in subnuclear structures. Using this technique, a PML body (arrow) demonstrates the characteristic decoration of the nuclear body by PML fringing its outer shell as well as positive staining for RNA throughout the entire nuclear body. As expected, RNA was also detected in nucleoli (N) and interchromatin granule (IG) regions. Chromatin surrounding the nucleolus is devoid of staining. (×20,600.)

the permeabilization of the cell membrane to enable uptake of Br-UTP may disrupt or be incompatible for proper RNA synthesis. To address this issue, we devised a new approach, not requiring permeabilization, in which nascent RNA is labeled by incorporation of a fluorescenated nucleotide (FITC–UTP) microinjected into living HEp-2 cells.

Immediately after microinjection of label (~5 min), cells are extracted of unincorporated FITC–UTP by a hypotonic-detergent solution, immunostained, and visualized for RNA incorporation by confocal fluorescence microscopy. Representative images shown in Fig. 1 *a*, *c*, and *e* display nucleoplasmic incorporation of the FITC–UTP with a limited number of larger and brighter discrete foci or nuclear domains. Ultimately, this label is largely redistributed into the cytoplasm (data not shown). In contrast to previously reported findings with Br-UTP labeling, nucleoli exhibit strong FITC–UTP incorporation in agreement with the expected high activity of RNA polymerase I. In addition to the bright nucleolar labeling, smaller foci similar in size to that of the PML-containing bodies can be seen above the homogeneous labeling of the nucleoplasm. As revealed in Fig. 1*b*, immunolabeling of these cells with antibodies to PML as a marker for the PML-containing nuclear body followed by imaging with confocal microscopy demonstrated that the majority of the FITC–UTP foci resides at this nuclear domain. Some of the PML-containing nuclear bodies did not colocalize with the FITC–UTP foci. Interestingly, a small number (two to four) of FITC–UTP foci did not colocalize with a PML-containing body. This prompted the examination of whether or not these foci colocalized with a different nuclear body. Accordingly, immunodetection of p80-coilin, which is a protein found in the nuclear domain termed the coiled body, was used to determine if these foci colocalized with the coiled body. Indeed, it appeared that some of the FITC–UTP foci colocalize with the coiled bodies (Fig. 1, *c* and *d*). This suggests the existence of at least two "classes" of foci that could be accounted for by either association with a coiled body or a PML-containing body. To determine if there might be an additional class of foci, cells were labeled with both PML and p80–coilin antibodies following FITC–UTP microinjection. Although there is an excess of immunoreactive bodies (PML and coiled) relative to fluorescent RNA foci, all RNA foci colocalized with either PML-containing bodies or coiled bodies (Fig. 1, *e* and *f*).

Immunoelectron Microscopy Identifies Ribonucleic Acid in the PML-Containing Bodies. Immunoelectron microscopy results show that PML is localized to the periphery of a spherical nuclear body with an electron-dense central core that lacks PML labeling (refs. 21 and 22; J.A.D. and R.L.O., unpublished observations). To confirm the presence of nucleic acid in the PML-containing nuclear body, we performed electron microscopic EDTA-regressive staining (36). This technique preferentially selects for staining of RNA rather than DNA and has been utilized to demonstrate RNA colocalization within nucleoli, interchromatin granular regions, and coiled bodies. Fig.

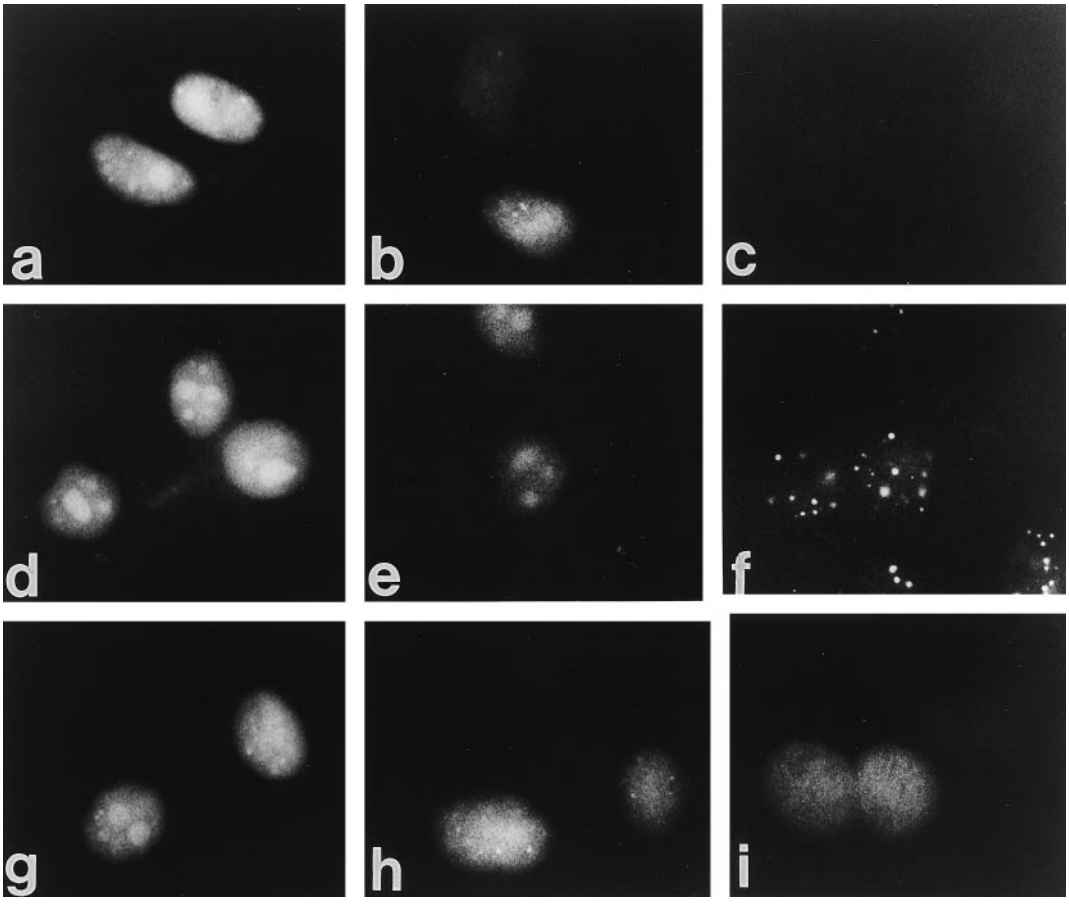

FIG. 3. Characterization of the FITC–UTP foci. When FITC–UTP is co-injected with increasing concentrations of unconjugated UTP, the fluorescent signal is competed away. The photomicrographs represent 0 (*a*), 50 (*b*) and 100 (*c*) mM UTP added along with 1 mM FITC–UTP. HEp-2 cells were nuclearly microinjected with 1 μg/ml of α-amanitin, and after 10 min, the cells were microinjected with FITC–UTP and then processed for microscopic evaluation. Compared with untreated control cells (*d*), microinjection of α-amanitin (*e*) inhibits the FITC–UTP labeling of foci and diminishes incorporation into the nucleoplasm but not nucleoli. A corresponding image of PML labeling (*f*) demonstrates that the structural integrity of the PML body is not affected by α-amanitin. The effect of actinomycin D-mannitol on incorporation of FITC–UTP was examined in cells incubated for 1 h at concentrations of 0 (*g*), 0.01 (*h*), and 0.20 (*i*) μg/ml. Actinomycin D appears to inhibit pol I synthesis at the lower dose and pol I and pol II at the higher dose.

2 shows RNA-positive structures including portions of the nucleolus (N), an interchromatin granular region (IG), and the PML-containing nuclear body revealed by immunogold-labeling with PML antisera (arrow). As expected, chromatin surrounding and within the nucleolus is virtually absent of staining. Taken together, these structural analyses, along with FITC–UTP foci corresponding to the PML-containing nuclear body, support the existence of nascent RNA within this nuclear domain.

Characterization of the FITC–UTP Foci. To confirm that the foci represented specific incorporation into RNA, unlabeled UTP was coinjected with the FITC–UTP. In a concentration-dependent fashion, FITC–UTP incorporation is chased by the unlabeled UTP as indicated by the progressive loss of foci, nucleolar labeling, and the generally diffuse labeling of the nucleoplasm (Fig. 3, *a*, *b*, and *c*). These data clearly support that the fluorescent moiety (FITC) does not create a labeling artifact. Other FITC-tagged reagents do not exhibit foci formation when introduced into the nucleus of a cell (V.J.L., unpublished observations). Additionally, microinjection of rhodamine-tagged 6-deoxy-UTP, which should not be incorporated into RNA, was not detected as foci, and when subjected to hypotonic extraction, essentially all of this fluorescence was removed. Furthermore, rhodamine 6-deoxy-UTP did not prevent the incorporation of FITC–UTP into RNA foci (data not shown).

RNA Foci, but Not Nucleoli, Are Sensitive to pol II Inhibitors. To determine the class of RNAs represented by the foci, the effects of a variety of compounds known to affect the synthesis of RNA were tested for their ability to inhibit FITC–UTP incorporation into nascent RNA. α-Amanitin, which selectively inhibits RNA pol II, was directly microinjected (1 μg/ml) into the nucleus of cells 10 min prior to re-injecting the same cells with FITC–UTP as described above. Whereas pol I nucleolar transcription was maintained, the diffuse nuclear incorporation was severely diminished, and foci were completely eliminated (Fig. 3*e*). It is of note that the microinjection of α-amanitin does not affect the immunostaining or integrity of the PML-containing bodies (Fig. 3*f*). Furthermore, these findings demonstrate that the PML-containing bodies do not simply serve as sites of excess UTP storage. Similarly, 0.2 μg/ml of actinomycin D-mannitol, known to inhibit pol II and pol I, affected the detection of FITC–UTP foci and overall incorporation (Fig. 3*i*), whereas lower doses known to selectively block pol I (0.01 μg/ml) affected incorporation only into the nucleoli (Fig. 3*h*). Taken together, these data suggest that the FITC–UTP RNA foci may be composed of RNA pol II transcripts and implicate the PML bodies in transcriptional processes.

The Coactivator CBP Colocalizes with the PML-Containing Nuclear Body. These results prompted us to examine whether or not regulatory factors known to be involved in transcriptional events colocalized with the PML body. As CBP has been demonstrated to serve as a cofactor for a wide variety of transcription factors, including hZIP proteins and nuclear receptors (30, 31), we examined whether it might, in part, be compartmentalized to the PML body.

Immunohistochemistry of the 265-kDa CBP protein demonstrated a largely heterogeneous, but nuclear, distribution of the protein in the cells (Fig. 4*b*) (29). Interestingly, utilizing an affinity-purified antibody directed against amino acids 634–648, which corresponds to a region of the CREB binding domain, endogenous CBP resides in a microparticulate pattern with a number of larger discrete foci reminiscent of the PML-containing nuclear body. This antibody is also a neutralizing antibody for CBP function as demonstrated previously (31). In this case, we find a strong colocalization of the coactivator CBP (Fig. 4*b*) with the PML-containing nuclear body as visualized with a monoclonal antibody detecting endogenous PML (Fig. 4*a*). Preabsorbing the CBP antibody with a peptide corresponding to the immunizing epitope resulted in complete loss of all CBP staining, confirming the specificity of the antibody (data not shown).

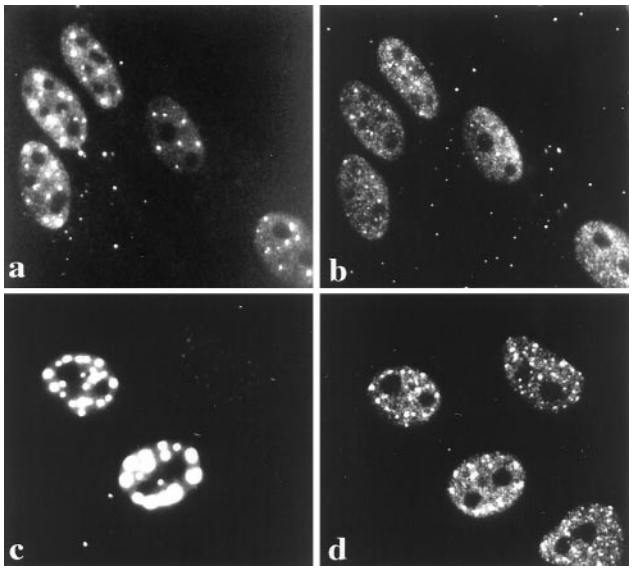

FIG. 4. CBP colocalizes with the PML-containing nuclear body. Double labeling of HEp-2 cells demonstrate PML-containing nuclear bodies as detected with the murine monoclonal antibody 5E10 (*a*). In the same cells, endogenous CBP is distributed in a finely speckled nucleoplasmic pattern as well as on larger nuclear foci, which can only be observed when utilizing the affinity-purified anti-CBP directed against amino acids 634–648 (*b*). Comparison of the images demonstrates that CBP and PML colocalize to the same nuclear bodies. To confirm this colocalization, cells exogenously expressing the PML-GFP fusion protein (*c*) were immunostained for CBP (*d*), which not only colocalized to the PML-containing nuclear body but appeared to label with a stronger signal, suggesting a recruitment of CBP to the PML bodies.

Overexpression of PML Recruits CBP to the Nuclear Bodies. To further confirm the validity of this colocalization, an expression plasmid encoding the PML-GFP fusion protein (40) was nuclearly microinjected into HEp-2 cells (Fig. 4*c*). Immunostained endogenous CBP colocalized to the PML-GFP labeled bodies (Fig. 4*d*). CBP-labeled domains appeared to be more prominent when PML was overexpressed, suggesting that PML may be recruiting CBP to the nuclear domain.

Immunolocalization studies of other antisera to CBP were performed. Polyclonal antibody (5729) to the N-terminal region (aa 1–100) yielded the same staining pattern and colocalization with PML-GFP. In contrast, polyclonal antisera (5614) to a glutathione *S*-transferase fusion of the KIX region of CBP (aa 455–679) and (C20) to a peptide corresponding to the C terminus of CBP (aa 2422–2441) only recognized the micropunctate CBP, which is scattered throughout the entire nucleoplasm and did not colocalize with PML–GFP and its corresponding nuclear body. Because of differences in the availability of epitopes and tertiary structure, it is not an unexpected finding that some of the antisera were able to discriminate between differentially localized CBP.

Immunoelectron Microscopic Localization of CBP to a Discrete Nuclear Body. To classically define and to further confirm that CBP resides in a nuclear body, immunoelectron microscopy was carried out using the affinity-purified anti-CBP antibody (634–648). Fig. 5*A* shows a discrete nuclear body labeled for CBP. Unlike the distribution of PML (Fig. 5*B*), CBP is not confined to the exterior shell of the body but is also found in the core. Differences in PML and CBP localization revealed only by immunoelectron microscopy may suggest inherently unique but co-participatory roles in the function of this nuclear body in transcription-related events.

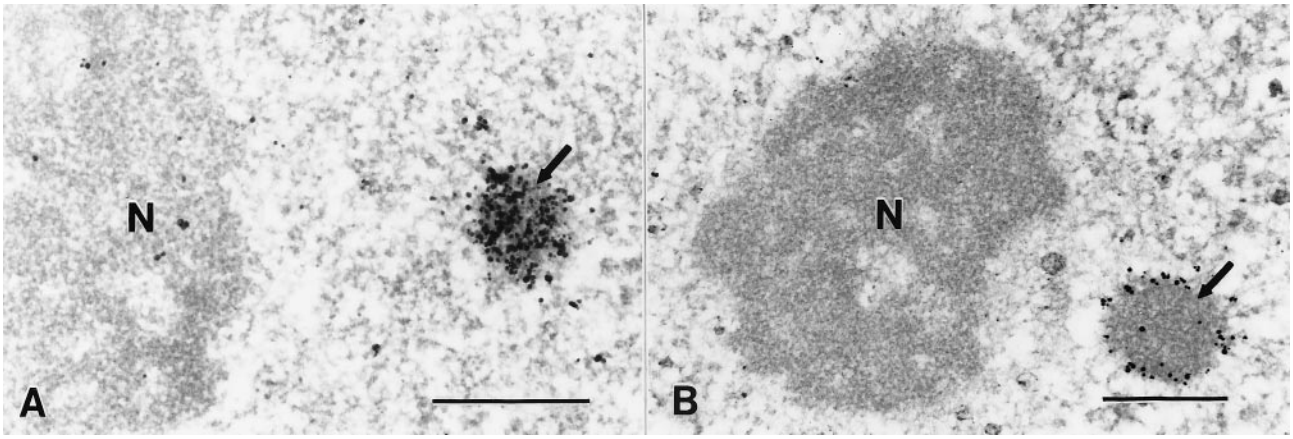

FIG. 5. Ultrastructural analysis of CBP and PML localization in HEp2 cells by immunoelectron microscopy. Silver-enhanced Nanogold pre-embedding immunoelectron microscopy (35) was performed utilizing affinity-purified rabbit antibodies to CBP (aa 634–648) and PML (aa 1–14). (*A*) CBP was localized in a nuclear body (arrow) with homogeneous labeling throughout. (*B*) PML localization was restricted to the outer shell of the PML-containing nuclear body (arrow). Nucleoli (N) were unlabeled. (Bar = 0.5 μm.)

DISCUSSION

There has been considerable effort in recent years to define a function for PML as well as its involvement in acute promyelocytic leukemia. The present findings have taken a different tack by identifying unique properties of the nuclear body itself where PML resides. By developing a new means of visualizing RNA, we have localized nascent RNA to the PML-containing nuclear body. Furthermore, these transcripts seem to be localized within the interior of the body at the ultrastructural level as seen by EDTA-regressive analysis. The absence of RNA foci with either α-amanitin or higher levels of actinomycin D treatment strongly support that these transcripts are products of RNA polymerase II. We cannot conclude that transcription is occurring at or within these sites. However, if the RNA is not produced there, it must arrive or be delivered immediately after transcription. A recent publication by Maul and coworkers (26) has localized viral transcripts next to the PML-containing nuclear body. Speculation could be made that perhaps these transcripts also reside in the body but are not easily detected as is likely the case with the Br-UTP detection. Coiled bodies have been shown to be involved in RNA processing and to contain RNA, in particular snRNA, which is transcribed by RNA polymerase II. Detection of nascent RNA in the coiled body is, however, a new finding. Interestingly, not all of the PML-containing nuclear bodies within a cell accumulate nascent RNA. This absence of uniformity suggests that not all of the PML bodies are equivalent and may have more than one functional state.

To further support a role for the PML-containing nuclear bodies in transcription-related events, we have discovered that the transcriptional cofactor, CBP, colocalizes with this body. It appears that expression of the PML protein constituent causes recruitment or further accumulation of CBP to these bodies, suggesting a potential physical association. Interestingly, the spatial distribution of CBP in the body is different from that of PML, suggesting that the interaction may be transient or indirect at the protein–protein level and that although they may reside in the same nuclear body ultrastructure (0.5 μm in diameter), their individual functions may be unique. Taken together, these findings provide an adumbration of the function of this nuclear body in transcriptional regulation. Future studies exploring the necessity of this body to the cell are underway by performing "structural knockouts," which inactivate the entire body rather than just a single protein.

We are indebted to Dr. M. H. Ellisman and Thomas J. Deerinck (Department of Neuroscience, University of California, San Diego) for their expertise and assistance in confocal microscopy performed at the San Diego Microscopy and Imaging Resource funded by National Institutes of Health Grant RR04050 and Dr. Tatiana Krasieva at the Laser Microbeam and Medical Program Resource funded by National Institutes of Health Grant RR01192. The CBP antibodies 5729 and 5614 were generously supplied by Dr. Marc Montminy. We also thank Dr. de Jong of the University of Amsterdam for 5E10 antibody and Dr. K. Umesono of Kyoto University for sharing the PML–GFP expression construct. This work was supported by Program Project CA54418 to R.M.E., who is an investigator of the Howard Hughes Medical Institute. V.J.L. is funded by the American Cancer Society, and J.A.D. is funded by a Walter Winchell–Damon Runyan Fellowship.

1. Guiochon-Mantel, A., Savouret, J., Quignon, F., Delabre, K., Milgrom, E. & De The, H. (1995) *Mol. Endocrinol.* **9,** 1791–1803.
2. Mu, Z. M., Chin, K. V., Liu, J. H., Lozano, G. & Chang, K. S. (1994) *Mol. Cell. Biol.* **14,** 6858–6867.
3. Rowley, J. D., Golomb, H. M. & Dougherty, C. (1977) *Lancet* **1,** 549–550.
4. de The, H., Chomienne, C., Lanotte, M., Degos, L. & Dejean, A. (1990) *Nature* **347,** 558–561.
5. Kakizuka, A., Miller, W., Jr., Umesono, K., Warrell, R., Jr., Frankel, S. R., Murty, V. V., Dmitrovsky, E. & Evans, R. M. (1991) *Cell* **66,** 663–674.
6. Borrow, J., Goddard, A. D., Sheer, D. & Solomon, E. (1990) *Science* **249,** 1577–1580.
7. Longo, L., Pandolfi, P. P., Biondi, A., Rambaldi, A., Mencarelli, A., Lo Coco, F., Diverio, D., Pegoraro, L., Avanzi, G., Tabilio, A., *et al*. (1990) *J. Exp. Med.* **172,** 1571–1575.
8. Goddard, A. D., Borrow, J., Freemont, P. S. & Solomon, E. (1991) *Science* **254,** 1371–1374.
9. de The, H., Lavau, C., Marchio, A., Chomienne, C., Degos, L. & Dejean, A. (1991) *Cell* **66,** 675–684.
10. Pandolfi, P. P., Grignani, F., Alcalay, M., Mencarelli, A., Biondi, A., LoCoco, F., Grignani, F. & Pelicci, P. G. (1991) *Oncogene* **6,** 1285–1292.
11. He, L. Z., Tribioli, C., Rivi, R., Peruzzi, D., Pelicci, P. G., Soares, V., Cattoretti, G. & Pandolfi, P. P. (1997) *Proc. Natl. Acad. Sci. USA* **94,** 5302–5307.
12. Brown, D., Kogan, S., Lagasse, E., Weissman, I., Alcalay, M., Pelicci, P. G., Atwater, S. & Bishop, J. M. (1997) *Proc. Natl. Acad. Sci. USA* **94,** 2551–2556.
13. Freemont, P. S. (1993) *Ann. N.Y. Acad. Sci.* **684,** 174–192.
14. Miki, T., Fleming, T. P., Crescenzi, M., Molloy, C. J., Blam, S. B., Reynolds, S. H. & Aaronson, S. A. (1991) *Proc. Natl. Acad. Sci. USA* **88,** 5167–5171.
15. Takahashi, M., Inaguma, Y., Hiai, H. & Hirose, F. (1988) *Mol. Cell. Biol.* **8,** 1853–1856.
16. Reddy, B. A., Kloc, M. & Etkin, L. (1991) *Dev. Biol.* **148,** 107–116.
17. Bellini, M., Lacroix, J. C. & Gall, J. G. (1993) *EMBO J.* **12,** 107–114.
18. Ben-Chetrit, E., Chan, E. K., Sullivan, K. F. & Tan, E. M. (1988) *J. Exp. Med.* **167,** 1560–1571.

19. Chan, E. K. L., Hamel, J. C., Buyon, J. P. & Tan, E. M. (1991) *J. Clin. Invest.* **87,** 68–79.
20. Dyck, J. A., Maul, G. G., Miller, W., Jr., Chen, J. D., Kakizuka, A. & Evans, R. M. (1994) *Cell* **76,** 333–343.
21. Koken, M. H., Puvion-Dutilleul, F., Guillemin, M. C., Viron, A., Linares-Cruz, G., Stuurman, N., de Jong, L., Szostecki, C., Calvo, F., Chomienne, C., *et al.* (1994) *EMBO J.* **13,** 1073–1083.
22. Weis, K., Rambaud, S., Lavau, C., Jansen, J., Carvalho, T., Carmo-Fonseca, M., Lamond, A. & Dejean, A. (1994) *Cell* **76,** 345–356.
23. Ascoli, C. A. & Maul, G. G. (1991) *J. Cell Biol.* **112,** 785–795.
24. Maul, G. G. & Everett, R. D. (1994) *J. Gen. Virol.* **75,** 1223–1233.
25. Ishov, A. M. & Maul, G. G. (1996) *J. Cell Biol.* **134,** 815–826.
26. Ishov, A. M., Stenberg, R. M. & Maul, G. G. (1997) *J. Cell Biol.* **138,** 5–16.
27. Arany, Z., Newsome, D., Oldread, E., Livingston, D. M. & Eckner, R. (1995) *Nature* **374,** 81–84.
28. Kwok, R. P. S., Laurance, M. E., Lundblad, J. R., Goldman, P. S., Shih, H., Connor, L. M., Marriott, S. J. & Goodman, R. H. (1996) *Nature* **380,** 642–646.
29. Chrivia, J. C., Kwok, R. P., Lamb, N., Hagiwara, M., Montminy, M. R. & Goodman, R. H. (1993) *Nature* **365,** 855–859.
30. Kamei, Y., Xu, L., Heinzel, T., Torchia, J., Kurokawa, R., Gloss, B., Lin, S. C., Heyman, R. A., Rose, D. W., Glass, C. K. & Rosenfeld, M. G. (1996) *Cell* **85,** 403–414.
31. Chakravarti, D., LaMorte, V. J., Nelson, M. C., Nakajima, T., Schulman, I. G., Juguilon, H., Montminy, M. & Evans, R. M. (1996) *Nature* **383,** 99–103.
32. Bannister, A. J. & Kouzarides, T. (1997) *Nature* **384,** 641–643.
33. Ogryzko, V. V., Schiltz, R. L., Russanova, V., Howard, B. H. & Nakatani, Y. (1996) *Cell* **87,** 953–959.
34. Raska, I., Andrade, L. E., Ochs, R. L., Chan, E. K., Chang, C. M., Roos, G. & Tan, E. M. (1991) *Exp. Cell Res.* **195,** 27–37.
35. Ochs, R. L., Stein, T., Jr. & Tan, E. M. (1994) *J. Cell Sci.* **107,** 385–399.
36. Bernhard, W. (1969) *J. Ultrastruct. Res.* **27,** 250–265.
37. Jackson, D. A., Hassan, A. B., Errington, R. J. & Cook, P. R. (1993) *EMBO J.* **12,** 1059–1065.
38. Wansink, D. G., Schul, W., van der Kraan, I., van Steensel, B., van Driel, R. & de Jong, L. (1993) *J. Cell Biol.* **122,** 283–293.
39. Grande, M. J., van der Kraan, I., van Steensel, B., Schul, W., de The, H., von der Voort, H. T. M., de Jong, L. & van Driel, R. (1996) *J. Cell. Biochem.* **63,** 280–291.
40. Ogawa, H., Inouye, S., Tsuji, F., Yasuda, K. & Umesono, K. (1995) *Proc. Natl. Acad. Sci. USA* **92,** 11899–11903.